

## Drug carrier in cancer therapy: A simulation study based on magnetic carrier substances

Tijjani Adam, Th S. Dhahi, Mohammed Mohammed, U. Hashim, N. Z. Noriman, and Omar S. Dahham

Citation: [AIP Conference Proceedings](#) **1885**, 020195 (2017); doi: 10.1063/1.5002389

View online: <http://dx.doi.org/10.1063/1.5002389>

View Table of Contents: <http://aip.scitation.org/toc/apc/1885/1>

Published by the [American Institute of Physics](#)

---

---

A promotional banner for AIP Conference Proceedings. The left side features a background of blue ocean waves with the text 'SUMMER SALE!' in large, bold, blue letters. Below this, the AIP logo (AIP |) is followed by 'Conference Proceedings' in a smaller blue font. The right side of the banner is a solid yellow triangle pointing left, containing the text '30% OFF ALL PRINT PROCEEDINGS!' in bold black letters. At the bottom of this yellow section, a white box contains the text 'ENTER COUPON CODE SUMMER2017' in black.

**SUMMER SALE!**

**30% OFF  
ALL PRINT  
PROCEEDINGS!**

**AIP | Conference Proceedings**

ENTER COUPON CODE  
SUMMER2017

# Drug Carrier in Cancer Therapy: A Simulation Study Based On Magnetic Carrier Substances

Tijjani Adam<sup>1,4,a)</sup>, Th S. Dhahi<sup>2,4,b)</sup>, Mohammed Mohammed<sup>3,c)</sup>, U. Hashim<sup>3,4,d)</sup>, N.Z Noriman<sup>1,e)</sup>, Omar S. Dahham<sup>1,f)</sup>

<sup>1</sup>*Faculty of Technology, Universiti Malaysia Perlis (UniMAP), Kampus Uniciti Alam Sg. Chuchuh, 02100 Padang Besar (U), Perlis, Malaysia*

<sup>2</sup>*Physics Department, College of Science Education, Basra University, Basra, Iraq*

<sup>3</sup>*Center of Excellence Geopolymer and Green Technology, School of Materials Engineering, Universiti Malaysia Perlis (UniMAP), 01007, P.O Box 77, D/A Pejabat Pos Besar, Kangar, Perlis, Malaysia.*

<sup>4</sup>*Institute of Nano Electronic Engineering (INEE), Universiti Malaysia Perlis (UniMAP), 01000 Kangar, Perlis, Malaysia*

Corresponding Author: <sup>a</sup>tijjani@unimap.edu.my

<sup>b</sup>sthikra@yahoo.com

<sup>c</sup>hmn7575@yahoo.com

<sup>d</sup>uda@unimap.edu.my

<sup>e</sup>niknoriman@unimap.edu.my

<sup>f</sup>eng.omar@mail.com

**Abstract.** The principle of magnetic carrier is a medium for transferring information by sending the drug to the specific part to kill tumor cells. Generally, there are seven stages of cancer. Most of the patient with cancer can only be detected when reaches stage four. At that stage, the cancer is difficult to destroy or to cure. Comparing to the nearly stage, there are probability to destroy tumor cell completely by sending the drug through magnetic carrier directly to nerve. Another way to destroyed tumor completely is by using Deoxyribonucleic acid (DNA). This project is about the simulation study based on magnetic carrier substances. The COMSOL multiphysic software is used in this project. The simulation model represents a permanent magnet, blood vessel, surrounding tissues and air in 2D. Based on result obtained, the graph shown during sending the magnetic flux is high. However, as its carry information the magnetic flux reduces from the above, the move from 0m until 0.009 m it become the lowers and start increase the flux from this until maximum at 0.018m. This is due the fact that carrier start to increase after because the low information is gradually reduce until 0.018m.

## INTRODUCTION

Today's technologies in medicine are widely grown especially in cancer therapy. There are many effective treatments such as surgery, chemotherapy, and radiation. The disadvantage of most chemotherapy is the relatively non-specific and cause side effects in healthy tissue. One of the ways to overcome this problem is by using a magnetic carrier. It can be retained at or guided to the target site by an external magnetic field of appropriate strength (Chertok *et al.*, 2011). Magnetic nanoparticles may open up a wide field of possible applications in medicine. Nowadays, magnetic nanoparticles have been used in medicine for magnetic separation techniques as contrast agents in magnetic resonance imagery, for local hyperthermia or as magnetic targetable carriers for various drug delivery systems (Tietze *et al.*, 2015). The magnetic carrier is one of applications in medicine to kill tumor in the cancer patient. Magnet is applied to send drug to the tumor.

Magnetic carrier made up from iron and carbon that attach to the anticancer agent and it will attract to the tumor by external magnetic field. This application in medicine is very important to reduce serious side effect. Usually, anticancer drugs can be delivered to cells in solid tumors by transport within a vessel, for example, blood circulation. Other ways are by transport across the vascular walls into surrounding tissues and through the interstitial space inside a tumor (Chertok *et al.*, 2011). Nowadays, there are many kinds of cancer treatment such as surgery, chemotherapy and radiation for cancer curing. However, these treatments have their limitations for example surgery. It can only treat a local tumor. Surgery may not be possible if the cancer has spread to other areas of the body or if the tumor cannot be removed without damaging vital organ such as the liver or brain. Besides that, chemotherapy also has their limitation. It can causes toxic side effect. Meanwhile, through radiation it can causes damage to normal tissues. As we are known after having cancer treatment many patients facing any side effect such as hair loss, nausea, vomit and others. Besides that, some of the treatment can cause damage to the normal tissues and also can cause lethal when using high dose. These magnetic carriers will need to be able to kill tumor without leaving any side effect, able to protect normal tissues from damage and able to avoid lethal while using high dose. Currently, most researchers are developing their structure or device without understanding parameter behavior that has great impact or influence on overall performance device. Every parameter has its own role. In the other hand, the use of in-situ in cancer treatment offers some exciting possibilities, including the possibility of destroying cancer tumors with minimal damage to healthy tissue and organs, as well as the detection and elimination of cancer cells before they form tumors. Most efforts to improve cancer treatment through nanotechnology are at the research or development stage. However the effort to make these treatments a reality is highly focused. For example, The Alliance for Nanotechnology in Cancer, established by the U.S. National Cancer Institute, is fostering innovation and collaboration among researchers to resolve some of the major challenges in the application of nanotechnology to cancer. In addition, there are many universities and companies worldwide working in this area. It is possible that these efforts will result in cancer becoming being nearly eliminated.

magnetic carrier, the advantages, current technology, limitation, magnetic drug delivery and the other research about magnetic carrier. At the present time, the using of magnetic carrier in cancer therapy has begun to be applied in the medical field especially in cancer treatment. Since, the using of magnetic carrier become an important technology in this century, various researches have been conducted to expand the area for further benefits. The use of magnetic carrier in cancer therapy is working when, the magnet is applied with the help of anticancer agent by external magnetic field. So, it will send drug to the affected area to kill tumors. In this way can ensure the drugs send only to the affected area only. Magnetic nanoparticles coated with chemotherapeutic agents have been used in clinical trials to concentrate medicine in narrow tumors by holding a single strong permanent magnet close to the skin surface (Komae, Member, & IEEE, 2016). This method also known as targeted magnetic drug delivery and can possibly improve the effectiveness of therapy and preserve the healthy tissues from the severe side effects of the managed drugs surface (Komae, Member, & IEEE, 2016). The contribution of nanomaterials in the delivery of anticancer drugs can improve the treatment effect by transporting the drugs to the target position and controlling the adverse receive by normal tissues. (Wu, et al., 2016). Current technology today use magnetic carrier based on biomedical application of magnetic nanoparticle. There are two types of application, inside (in vivo) and outside (in vitro) the body. In vivo applications, it separated in therapeutic (hyperthermia and drug- targeting) and diagnosis application (nuclear magnetic resonance (NMR) imaging). While, in vitro application is diagnostic (separation/selection, and magnetorelaxometry) (Lyer *et al.*, 2007). Recent research, based on phantom studies and preclinical studies, has shown that the magnetic resonance imaging (MRI) could be employed to navigate drug-loaded magnetic particles to deep-seated lesions in the human body having a targeting accuracy that is limited only by the voxel size of the MRI scanner ( Vartholomeos, Member, IEEE, & Mavroidis, 2012). The application of this method in clinical cases would increase the drug concentration at the lesion and thus its therapeutic efficiency, while at the same time would reduce the side effects on the healthy tissues ( Vartholomeos, Member, IEEE, & Mavroidis, 2012).The progress of composite systems of magnetic nanoparticles and block copolymers deals with the potential for magnetic field-triggered drug release, which consumes localized heating to cause phase separation or melting within the polymericcarrier (Glover, et al., 2013). The using of magnetic carrier in cancer therapy offering advantage such as, the ability to target specific locations in the body, the reduction of the quantity of drug needed and the reduction of the concentration of the drug at the non-target site and also minimizing severe side effect (Jurgons *et al.*, 2007). In the era of nanotechnology today, magnetic nanoparticle is attracting increasing attention because of opportunities in cancer therapy (Jurgons *et al.*, 2007). Nanoparticle have unique physical and chemical properties due to their size, which is in

the same range as antibodies, receptors, nuclei acid, proteins and other biological macromolecule (Lyer *et al.*, 2007). Regarding to the therapeutic applications, drug transportation in a nanoparticle bound form enables even less soluble or instable agents to reach tumor cells (Lyer *et al.*, 2007).

However, in recent technology nowadays there are still having some limitation in cancer therapy by hyperthermia, drug targeting via thermosensitive magnetic nanoparticle MNP and the application of magnetically controllable catheters (Hergt *et al.*, 2007). It is desirable to realize the temperature enhancement needed for a special application with as low as possible amount of MNP, meaning that the heat power generated per particle unit mass should be as high as possible. This is most important for applications where target concentration is very low as for instance in antibody targeting of tumors (Hergt *et al.*, 2007). Taking into account the heat depletion into the tumors surrounding it is shown that the therapeutic particle concentration at the tumor site is crucially related to the tumor size. Consequences of inhomogeneities of particle supply as well as non-reproducibility of physical particle parameters for therapy risks are considered (Hergt *et al.*, 2007). There is well-known trust that many solid carcinomas will be well cured using nanocarriers encapsulating a cancer drug, due to their greater capability to focus drug delivery into the tumor and considerably avoid delivery to other tissues (Siegel *et al.*, 2016). Drug delivery systems incline to use magnetic particles which are very effective, but they can't always be used because these particles can be toxic in certain physiological conditions (Agila & Poornima, 2015). In contrast, graphene doesn't have any magnetic properties; also can be altered into liquid crystal simply and cheaply strengthening the view that it may be used for a new kind of drug delivery system (Agila & Poornima, 2015). Combination of a controlled polymeric drug delivery system with Magnetic Nanoparticles (MNPs) opens up a new method to target the carcinoma cells (Kini, Bahadur, & Panda, 2011). There are numerous types of polymeric drug delivery systems. For example biodegradable and biocompatible polymeric system [poly (DL-lactide-co-glycolide) (PLGA)] has been found to play an important role as a drug delivery system (Kini, Bahadur, & Panda, 2011).

For tumor cells, involving chemotherapeutic agents to minor superparamagnetic particles and pointing them over the bloodstream to the affected area with the help of external magnetic fields has shown promising results and has already been successfully tested clinically. Even gene transfection in endothelium cells with magnetic nanoparticles has been successfully presented recently (Goetz *et al.*, 2010). An earliest experimental arrangement for magnetic drug targeting in the lung has been presented in and started a fresh field of research subsequently. Based on the experimental setup, by Dames *et al.*, the nebulized drug solvents have been marked with slight coated magnetite particles. These inhaled aerosol droplets were focused with a permanent magnet inside the lungs of mice (Goetz *et al.*, 2010). One of the important differences between air and liquid-like blood are having smaller viscosity. Tribologic parameter controls the acceleration of particles through a magnetic gradient field, it is markedly easier to concentrate nanomagnets with smaller external field characteristics compared to magnetic drug targeting in the blood stream. This is an important concern for the possible operating range of the externally generated magnetic field in the body (Goetz *et al.*, 2010). Soltani et al studied the effect of tumor shape and size on drug delivery by modeling interstitial fluid flow and assuming that drug particles flow in the interstitial fluid. The interstitial velocity in tumors goes to zero and pressure differences are minimum in large tumor (order of 10 cm<sup>3</sup>). Therefore, the effect of convection transport is reduced and sometimes insignificant in large tumors. In the lung tumors, the size involve is large, drug delivery is only depends on diffusion mechanisms, and size of tumors does not affect drug delivery. Meanwhile, for the hypothetical tumor, the size is small. So, the effect of convection transport is higher than in larger tumors. Then the drug delivery is increasing in small tumors is greater than in large tumors (Soltani et al., 2015).

## METHODS

This process includes two steps which are schematic design and implements numerical calculation. First of all, before design schematic the model parameter must be identified. This model parameter will ensure the simulation will be done successfully. Next, implementation of numerical calculation is done by solving the Maxwell's equations for a static magnetic field. The resulting magnetic field is coupled to a fluid flow problem described by the Navier Stokes equations. By adding a magnetic volume force, which stems from the solution to the magnetic field problem, to the Navier Stokes equations, ferrohydrodynamics of the blood can be studied. After that, the schematic can be design and simulate by using COMSOL Multiphysics software.

COMSOL Multiphysics software is often used for designing. This software can use to design in 2D or 3D form, but for this project 2D is used. There are several functions that are available in this software that will be

used in this project. Besides that, there are some step that must follow by using this software. The first step is model navigator, after open the software the first view is model navigator. From here 2D is selected in space dimension. Incompressible Navier-Stokes and Magnetostatics was added. The second step is geometry modelling. In this geometry modelling, rectangular shape is used. The value of weight, height, base x and base y was inserted in the dialog box. After that, zoom extents and fillet/chamfer was used to insert value of radius. In this step three arbitrary rectangular were draw and insert the different value of height and base y. Zoom extent was used two times in this step. The third step is option and setting. From these step, the constant value was inserted includes names, expressions (values and units), and descriptions (the descriptions are optional). Besides, the scalar expression was inserted in this step. The fourth step is physics setting. In this physics setting step, there are some steps involves such as application mode properties, subdomain setting and boundary setting for magetostatics and navier stokes. For application mode properties, the properties were chosen from physics menu. Then, the default element was changing to lagrange - cubic in application mode properties. Whereas, for subdomain and boundary setting, the different parameter are inserted in the subdomain setting dialog box and boundary setting dialog box. For subdomain setting – magnetostatics , subdomain 2 was selected in physics page and then the constitutive relation was set to  $B = \mu_0 H + \mu_0 M$ . After that, the subdomain 5 was selected and then the constitutive relation was set to  $B = \mu_0 \mu_r H + B_r$  and then enter  $\mu_{r\_mag}$  in  $\mu_r$  edit field. While,  $B_{rem}$  was entered in the right  $B_r$  edit field for the  $y$ -component of the remanent flux density, and leave the corresponding  $x$ -component at zero. Firstly, incompressible Navier – Stokes was chosen from Multiphysics menu and then the subdomain setting was chosen from physics menu. After that, all five subdomain was selected and clear the active in this domain. Next, subdomain 2 and active in this domain was selected and enters the fluid properties according to the table below. After enter the fluid properties, Artificial Diffusion button was clicked to add streamline diffusion to the model. This is necessary because of the high Reynolds number flow. Then, on the init page, all initial conditions leave at zero. Boundary setting is chosen from physics menu and enters the specific boundary condition according to the following table. The fifth step is mesh generation. Free Mesh Parameter was chosen through Mesh toolbar. After that, subdomain 2 was selected and value of 0.002 was entering in the maximum element size. The result obtain is shown in above figure after finish mesh. The six step is computing the solution, in this step solver manager button was clicked through solve for toolbar and magnetostatics. After that, solver parameter was clicked through general, stationary and analysis toolbar. Lastly, solve by using solve button. The last step is the postprocessing and visualization, in this step the plot parameter button is used to generate the figure. Besides, Magnetic flux density norm was chosen on surface data. Meanwhile, Magnetic potential, z component was chosen on contour page. The below is the result from this final step.

## RESULTS AND DISCUSSION

Magnetic flux is a measurement of the total magnetic field which passes through a given area. Moreover, the effect of the magnetic forces able to distinguish. Around the magnet there is a magnetic field and this gives a ‘flow of magnetic energy’ around the magnet. This flow of energy is called magnetic flux ( $\Phi$ ). From the figure above, the magnetic flux as flowing from the north pole of a magnet round to south pole as shown by the arrows on the lines in the figure. Based on figure below, the flux flowing as much from north pole as there is flowing into south pole.

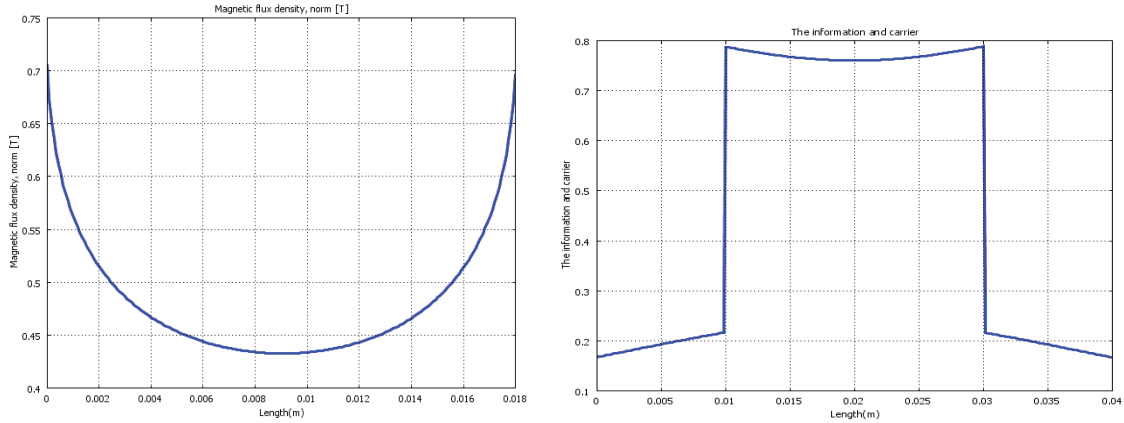


**FIGURE 1.** (a)The magnetic flux density with the distance of carrier move at the upper part of cross sectioning (b) The information and carrier with the distance of carrier move at the middle part cross sectioning.

From figure 1 the graph shown when the magnetic flux increase the distance is increasing. This is because when the magnetic flux reach in the specific region, it became decrease and then increase when further from the region. Generally, the magnetic flux solely the carrier, during sending the magnetic flux is high. However, as its carry information the magnetic flux reduces form the above, the move from 0m until 0.009 m it become the lowest and start increase the flux from this until maximum at 0.018m. This is due the fact that carrier start to increase after because the low information is gradually reduce until 0.018m. From figure 4.3, the graph shown the information is increasing from 0m to 0.010m and continues increasing at 0.010m with the maximum information. At that point it became reduced to 0.020m and continue increasing until 0.030m. At that point the information is drop and start reducing until 0.040m.

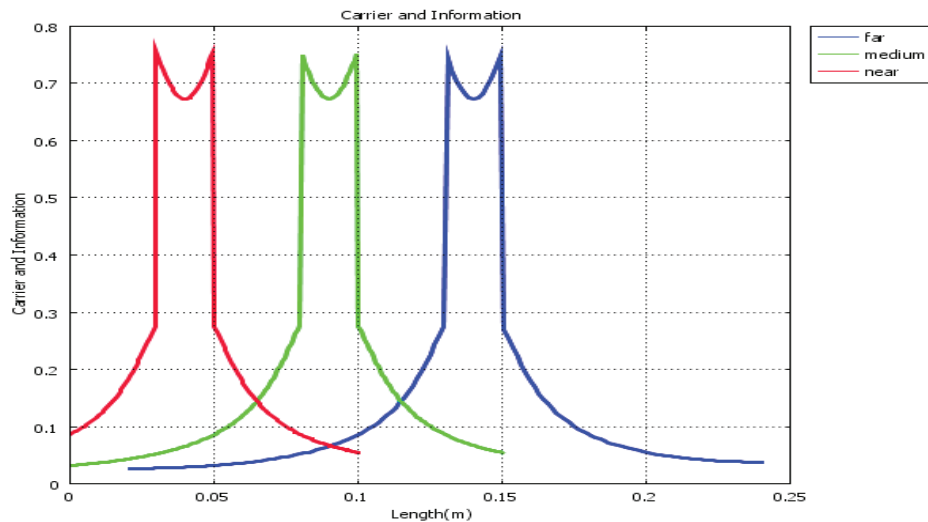


**FIGURE 2.** The information and carrier with the distance of carrier move at the different length cross sectioning.

From figure 2, the graph shown the blue colour indicates the behavior at far, the green colour is medium while red colour at near length. From the result obtained the blue colour indicate the information that carried is lower than green and red colour from starting point and became increase until 0.130m and the information continuous increase rapidly at that point and became reduce to 0.140m and increase back until 0.150m and drop rapidly at 0.150m and became reduce until 0.240mm.

For green colour, the information that carried is greater than blue colour from starting point and became increase increase until 0.070m and continue increasing rapidly at that point and became reduce to 0.090m and increase back until 0.1m and drop rapidly from that point and became reduce until 0.150m. For red colour,

the information that carried is greater than blue and green colour from starting point and became increase until 0.250m and continue increasing rapidly at that point and became reduce to 0.040m and increase back to 0.050m and drop rapidly from that point and became reduce until 0.1m. For difference graph of difference parameter at the different length cross sectioning can refer to Appendix C (i) From the figure 4.5, the graph shown at the starting point the information is lower. So, the carrier is increasing from 0m until 0.0018m. Meanwhile, from the figure 4.6 at the starting point the information is high. So, the carrier is reduce from 0m until 0.0085m and continue increase from that point until maximum at 0.018m. when the distance also increase until maximum value.

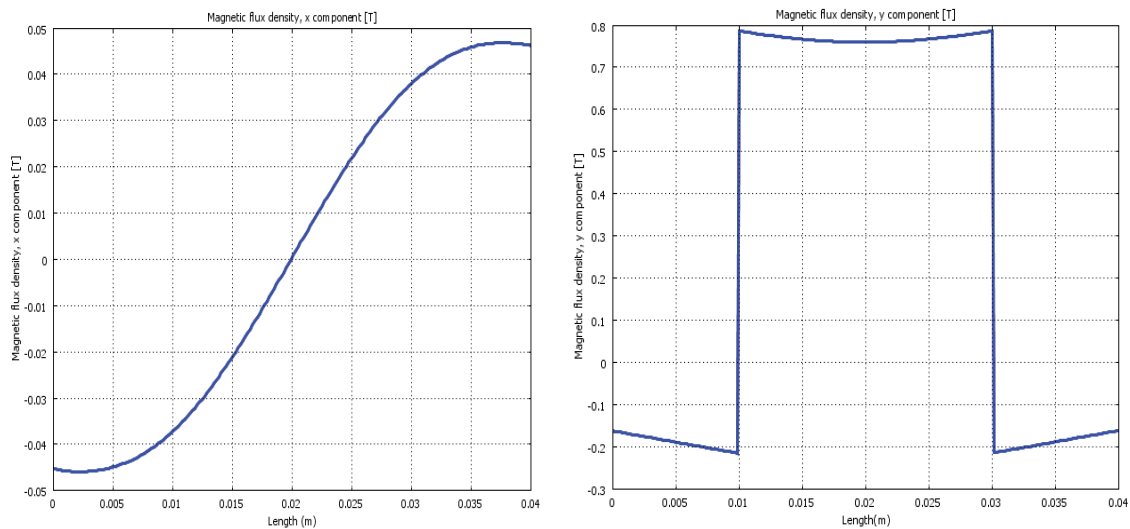


**FIGURE 3.** (a) The magnetic flux density,x component with the distance of carrier move at the middle part of cross sectioning (b) The magnetic flux density,y component with the distance of carrier move at the middle part of cross sectioning.

From the figure 3, the graph shown during sending, the information is high. So, the carrier with is magnetic flux is reduce from 0m until 0.0045m and than become increase until 0.0355m and became reduce at that point until 0.004m due to the high information at the end. As comparisons, from figure 4.8 the graph shown during the sending the information is high.so, the carrier is reduce to 0.01m and as the information is low, the carrier increase rapidly at that point and become reduce until 0.02m and increase back from that point until 0.03m. At that point the carrier is drop rapidly and became increase until 0.04m.

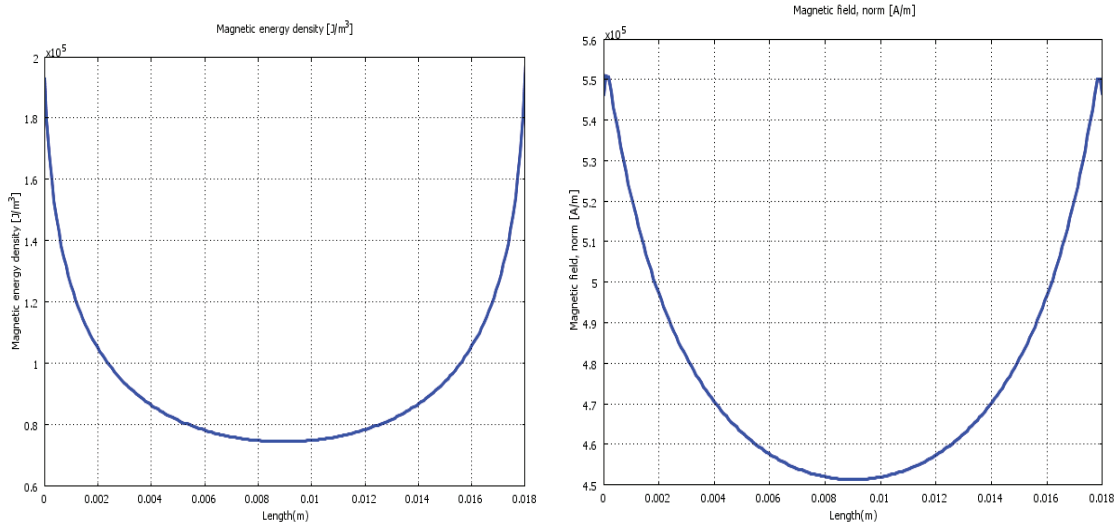


**FIGURE 4.** (a) The magnetic energy density, with the distance of carrier move at the upper part cross sectioning (b) The magnetic field, with the distance of carrier move at the upper part cross sectioning.

From figure 4, the graph shown that, the carrier that is magnetic energy density is reduce from 0m until 0.0085m when the information is high at the starting point. The carrier continue to increase from 0.0085m until 0.018m. While, from figure 4.10 the carrier (magnetic field) is reduce faster that figure 4.8 at the starting point from 0m until 0.0085m. After that, the carrier continue increase faster at that point until 0.018m.

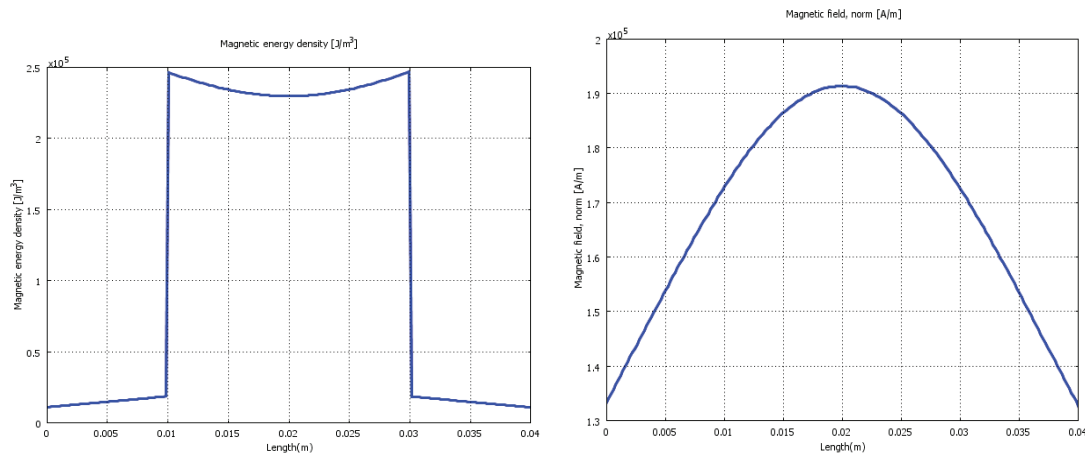


**FIGURE 5.** (a) The magnetic energy density, with the distance of carrier move at the middle part cross sectioning (b) The magnetic field, with the distance of carrier move at the middle part cross sectioning.

From figure 5, the graph shown that the carrier that is magnetic energy density at starting point is increasing from 0m until 0.010m and became increase rapidly at that point due to low information. After that, the carrier became reduce until 0.020m and increase back from that point until 0.030m. At that point the carrier is drop rapidly due to high information and became reduce back until 0.040m. Meanwhile, from figure 4.12, the graph shown at the starting point the carrier that is magnetic field is increase from 0m until 0.020m and continue decrease from that point until 0.040m.

### Implement numerical calculation

In this calculation involved two equation Magnetostatics and Fluid Flow equation.

- **Magnetostatics equations**

Maxwell's equation was applied for magnetic field  $\mathbf{H}$  (A/m) and the current density  $\mathbf{J}$  (A/m<sup>2</sup>)

$$\nabla \times \mathbf{H} = \mathbf{J} \quad (1)$$

Besides, Gauss' law for the magnetic flux density  $\mathbf{B}$  (Vs/m<sup>2</sup>) was stated as below:

$$\nabla \cdot \mathbf{B} = 0 \quad (2)$$

The equation below is the constitutive equations describing the relation between  $\mathbf{B}$  and  $\mathbf{H}$  in the different parts of the modeling domain:

$$\mathbf{B} = \begin{cases} \mu_0 \mu_r \text{mag}H + B_{rem} & \text{permanent magnet} \\ \mu_0 (H + M_{ff}(H)) & \text{blood stream} \\ \mu_0 H & \text{tissues and water} \end{cases} \quad (3)$$

Magnetic vector potential  $\mathbf{A}$ :

$$\mathbf{B} = \nabla \times \mathbf{A}, \quad \nabla \cdot \mathbf{A} = 0 \quad (4)$$

Substitute the Equation 3 into equation 1. Then, solve the vector equation below:

$$\nabla \times \left( \frac{1}{\mu} \nabla \times \mathbf{A} - \mathbf{M} \right) = \mathbf{J}$$

After 2D problem was simplify with no perpendicular currents, this equation become:

$$\nabla \times \left( \frac{1}{\mu} \nabla \times \mathbf{A} - \mathbf{M} \right) = 0 \quad (5)$$

Assumes the equation that, the magnetic vector potential has a nonzero component only perpendicularly to the plane,  $\mathbf{A} = (0, 0, A_z)$ .

Two material parameters  $\alpha$  (A/m) and  $\beta$  (m/A) of arc tangent expression characterizes the induced magnetization  $\mathbf{M}_{ff}(x, y) = (M_{ffx}, M_{ffy})$  of a ferrofluid

$$\begin{aligned} M_x &= \alpha \text{atan} \left( \frac{\beta}{\mu_0} \cdot \frac{\partial A_z}{\partial y} \right) \\ M_y &= \alpha \text{atan} \left( \frac{\beta}{\mu_0} \cdot \frac{\partial A_z}{\partial x} \right) \end{aligned} \quad (6)$$

where  $\chi = \alpha\beta$  is the magnetic susceptibility.

- **Fluid Flow Equations**

The Navier-Stokes equations describe the time-dependent mass and momentum balances for an incompressible flow:

$$\begin{aligned} \rho \frac{\partial \mathbf{u}}{\partial t} - \nabla \cdot n(\nabla \mathbf{u} + (\nabla \mathbf{u})^T) + \mu \mathbf{u} \cdot \nabla \mathbf{u} + \nabla p &= \mathbf{F} \\ \nabla \cdot \mathbf{u} &= 0 \end{aligned} \quad (7)$$

With the assumption that the magnetic nanoparticles in the fluid do not interact, the magnetic force  $\mathbf{F} = (F_x, F_y)$  on the ferrofluid for relatively weak fields is given by  $F = |M| |\nabla H|$ , by using the above equation (3), (4), and (6) then come out to the expressions:

$$F_x = \frac{x}{\mu_0 \mu r^2} \left( \frac{\partial A_z}{\partial x} \cdot \frac{\partial^2 A_z}{\partial x^2} + \frac{\partial A_z}{\partial y} \cdot \frac{\partial^2 A_z}{\partial x \partial y} \right)$$

$$F_y = \frac{x}{\mu_0 \mu r^2} \left( \frac{\partial A_z}{\partial x} \cdot \frac{\partial^2 A_z}{\partial x \partial y} + \frac{\partial A_z}{\partial y} \cdot \frac{\partial^2 A_z}{\partial y^2} \right)$$

The Difference Parameter at the Different Length Cross Sectioning

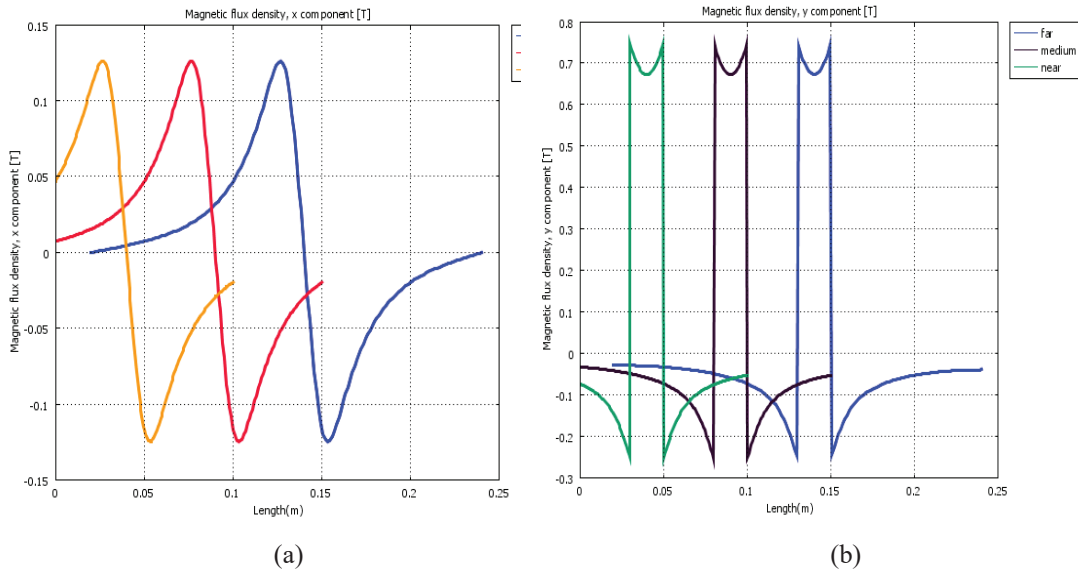


FIGURE 6. (a)The magnetic flux density, x component with the the distance of carrier move at the different different length cross sectioning (b) The magnetic flux density, y component with the distance of carrier move at the different length cross sectioning

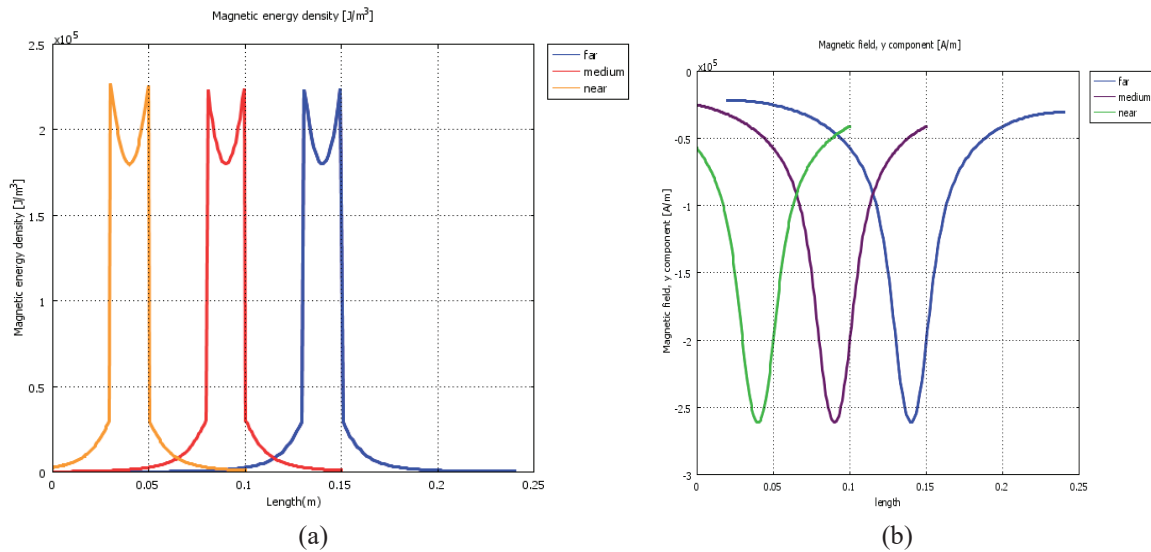


FIGURE 7. (a)The magnetic energy density with the distance of carrier move at the different length cross sectioning at the different length cross section (b) The magnetic field, y component with the distance of carrier move at the different length cross sectioning

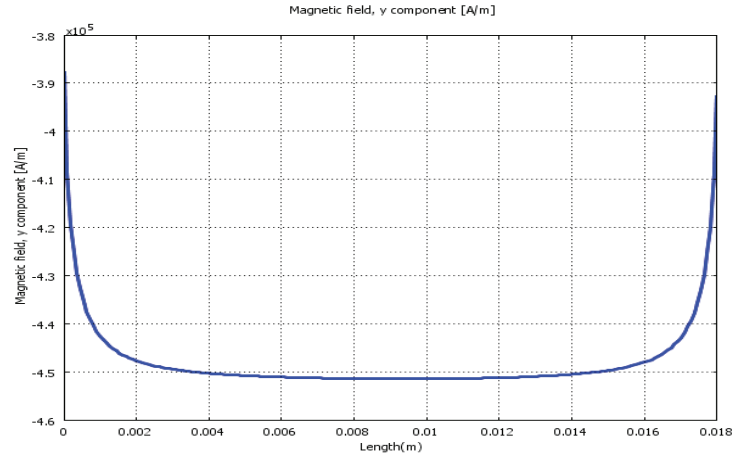


FIGURE 8. The magnetic field,y component with the distance of carrier move at the upper part cross sectioning.

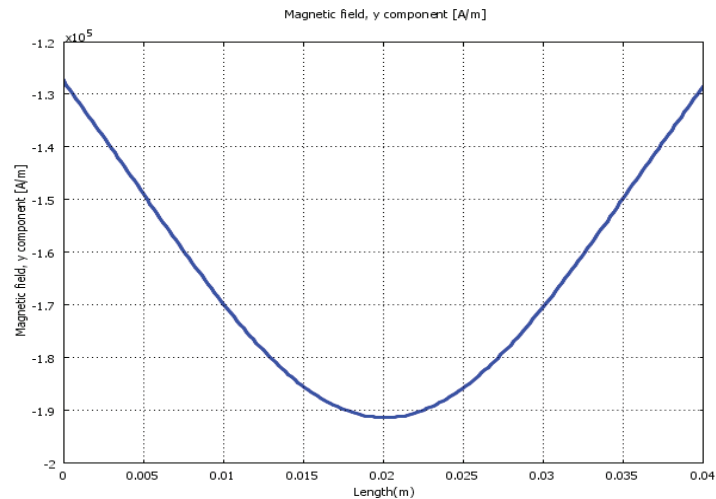


FIGURE 9. The magnetic field,y component with the distance of carrier move at the middle part cross sectioning.

## CONCLUSION

In this project, all the objectives are achieved. Firstly, the simulations parameters are identified, such as geometric parameter, constant value, scalar expression, fluid properties, pressure, velocity and many others. For the geometric parameter the shape and size are determined. Secondly, the model schematics are designed completely using COMSOL Multiphysics software. Third, the numerical calculation was successfully implemented. Forth, the parameter performance was observed by changing some of the parameter. The performance of carrier move can be observed by the obtained graph.

## REFERENCE

1. S. Agila and J. Poornima, "Magnetically Controlled Nano-Composite Based 3D Printed Cell Scaffolds As Targeted Drug Delivery Systems For Cancer Therapy," *IEEE International Conference on Nanotechnology* (IEEE International Conference on Nanotechnology, Italy, 2015) pp.1058-1061.
2. B. Chertok, E. Allan David and Victor C. Yang, *J. Control. Release*, 393-399 (2011).
3. A. L. Glover, J. B. Bennett, J. S. Pritchett, S. M. Nikles, D. E. Nikles, J. A. Nikles, and C. S. Brazel, *IEEE Trans. Magn.*, 231-235 (2013).
4. S. M. Goetz, C. Dahmani, C. Rudolph and T. Weyh, *IEEE Trans. Biomed. Eng.*, 2115-2121 (2010).
5. R. Hergt and S. Dutz, *J. Magn. Magn. Mater.*, 187-192 (2007).

6. T. K. Indira and P. K. Lakshmi, International Journal of Pharmaceutical Science and Nanotechnology, 1035-1042 (2010).
7. R. Jurgons, C. Seliger, A. Hilpert, L. Trahms, S. Odenbach and C. Alexiou, *J. Phys. Condens. Matter.*, 2893-2902 (2006).
8. S. Kini, D. Bahadur and D. Panda, *IEEE Trans. Magn.*, 2882-2886 (2011).
9. A. Komace, Member and IEEE, *IEEE Trans. Control Syst. Technol.*, 129-144 (2016).
10. P. Kopcansky, M. Timko, M. Hnatic, M. Vala, G. M. Arzumanyan, E. A. Hayryan, J. Chovanak, Communication of the Joint Institute for Nuclear Research, 1-13 (2009).
11. M. Lohakan, C. Yensiri, S. Boonsang and C. Pintavirooj, Research Publishing Services, 467-470 (2006).
12. T. Lunnoo and T. Puangmali, *Nanoscale Res. Lett.*, 1-11 (2015).
13. G. U. Marten, T. Gelbrich, H. Ritter and A. M. Schmidt, *IEEE Trans. Magn.*, 364-372 (2015).
14. S. Sharma, A. Gaur, U. Singh and V. K. Katiyar, Recent Advances in Fluid Mechanics and Thermal Engineering, 116-120 (2014).
15. R. A. Siegel, A. R. Kirtane and J. Panyam, *IEEE Trans. Biomed. Eng.*, 11 (2016).
16. M. Soltani, M. Sefidgar, H. Bazmara, C. Marcus, R. M. Subramaniam and A. A. Rahmim, *IEEE PDFeXpress*, 1-6 (2015).
17. R. Tietze, J. Zaloga, H. Unterweger, S. Lyer, R. P. Friedrich, C. Janko, C. Alexiou, *Biochem. Biophys. Res. Commun.*, 463-470 (2015).
18. P. Vartholomeos, IEEE Member and C. Mavroidis, *IEEE Trans. Biomed. Eng.*, 3028-3038 (2012).
19. J. Wu, A. Deng, W. Jiang, R. Tian, W. Jiang and Y. Shen, "Synthesis and characterization of pH-sensitive magnetic," *Proceedings of the 16th International Conference on Nanotechnology* (Sendai: IEEE International Conference on Nanotechnology 2016) pp. 543-546.
20. J. Zhang, C. Q. Lan, M. Post, B. Simard, Y. Deslandes and T. H. Hsieh, *Cancer Genomics Proteomics*, 147-158 (2006).